Thermal and structural properties of ZnO-Bi$_2$O$_3$-B$_2$O$_3$ glasses doped with NiO

S. Patel[1], B. Fageria*[,1],
K.S. Gill[2], S. Soni[1], V.N. Mishra[3]

[1]Dr Harisingh Gour Vishwavidyalaya, Sagar, India

[2]Government College Hisar, Haryana, India

[3]Indira Gandhi National Tribal University, Amarkantak, India

E-mail: bluwileyq@gmail.com

Among new low melting glasses, bismuthate glass is deemed to have the most potential. Current studies of these glasses focus on the thermal and structural influence of the additional oxide (NiO). The glass transition temperature, T_g and peak crystallization temperatures(T_{p1} and T_{p2}) was studied in all samples using a differential scanning calorimeter. We found that the glass transition temperature and crystallization temperature increases with the increase in the content of NiO. Further, NiO-ZnO-Bi$_2$O$_3$-B$_2$O$_3$ glasses were investigated spectroscopic ally with Fourier-Transform Infrared (FTIR) spectra recorded for glass with different main oxide contents. The formation of B-O-Bi and B-O-Zn/Ni bridging bonds in the glass structure is suggested from FTIR spectra. In the present work, the thermal and structural properties of zinc bismuth borate glasses doped nickel ions have been carried out.

Keywords: transition temperature; crystallization; differential scanning calorimeter; FTIR

Introduction

The early research on bismuth-borate glass was of great importance because it first attempted to systematically study the relationship between a glass's composition and its physical and chemical properties. It also demonstrated the wide range of compositions that would form glasses [1]. ZnO is an essential additive that acts to reduce the melting points in the oxides glass matrix formation. Here ZnO

is chosen to modify some of structural and thermal properties. While NiO was introduced to modify the stability, to enhance the amorphousity of matrix, and help in the melting of all batch components (i.e. Bi_2O_3, B_2O_3, and ZnO) and force some of the Zn^{2+} cations to share in the glass matrix as glass network formers of tetrahedral coordination states [2]. B_2O_3 is one of the most common glass formers because molten B_2O_3 does not crystallize by itself even when cooled at the slowest rate [3-7]. According to Krogh-Moe [3], the arrangement of vitreous B_2O_3 consists of a random network of boroxyl rings and BO_3 triangles connected by B-O-B linkages. Borate glasses could transform the triangular BO_3 units to BO_4 tetrahedra with a coordination number four [4]. It is reported that Bi_2O_3 has a solid effect of lowering the melting temperatures in various glass matrix [8]. In Bi_2O_3 -based glasses, the bismuth ions may appear in BiO_3 pyramidal and BiO_6 octahedral units [5, 6]. It is well known that structural stability has a crucial influence on the properties of the materials. Building a connection between structural and crystallization of NiO-ZnO-Bi_2O_3-B_2O_3 should be of great importance for better understanding this material's thermal and structural properties. The present work will concentrate on modern aspects of the application of Bismuth Borate Glasses containing Nickel oxide in the fields of optics and related techniques together with their structural basis.

Experimental procedure

A series of four glass samples of formula xNiO-(20-x)ZnO-$40Bi_2O_3$-$40B_2O_3$; where x= 0, 0.5, 1.0 & 2.0 mol% were prepared by using the conventional melt quenching Method. The required amount of chemicals, zinc oxide (ZnO, purity $\geq$ 99%, Merck), bismuth oxide (Bi_2O_3, purity $\geq$ 99.99%, Sigma-Aldrich), boric oxide (B_2O_3, purity $\geq$ 99.98%, Sigma-Aldrich), and nickel oxide (NiO, purity $\geq$ 99%, Rankem) all were Weighed and mechanically mixed in an agate pestle-mortar to obtain a fine powder. The obtained mixture was melted in a High-Grade Alumina Crucibles (Ants Ceramics) in a muffle furnace at a temperature of $1100°C$ for 2 Hours. Then these melt are poured on a brass plate maintained at $0°C$ to perform the quenching because at room temperature outer surface of glass will quench more rapidly than the inner surface. This may result in the crystallization of inner surface of glass after than these glasses were annealed at $250°C$ for about 6 hours to eliminate thermal stresses. All samples were coded as seen in Table 1.

Table 1.
Samples code and oxides ratios.

Code	The Ratio of each component in mol%			
	ZnO	Bi_2O_3	B_2O_3	NiO
N_0	20	40	40	0.0
$N_{0.5}$	19.5	40	40	0.5
$N_{1.0}$	19	40	40	1.0
$N_{2.0}$	18	40	40	2.0

The amorphous nature of all the samples was confirmed by the absence of Bragg's peak in the X-ray diffraction pattern. The glass transition temperature, T_g, was studied in all samples using a differential scanning calorimeter (TA Instruments). All the glass batches were heated at the standard rate of $10°C$ min^{-1} up to $800°C$ in alumina pans. FTIR spectra were used to identify structural stability and bond formation within the glass matrix, at room temperature, using Fourier transform Infrared (FTIR) spectrometer in the range from 2000 to 400 cm^{-1}. Where, the powdered samples were mixed well with KBr and were then pressed to make pellets suitable for IR measurements. Since, each FTIR band composed of more than one peak, each represents a fixed type of vibration, it should be de-convoluted each band by separating all possible individual peaks.

Result and discussion

XRD Characterization

Figure 1 shows as deposited XRD for all studied samples, from $10°$ to $80°$ at $1°$/minute respectively. These graphs demonstrated all studied glass matrix did not show any Bragg's peaks and, only two extensive humps around $29.5°$ and $51.8°$ are detected; such humps distinguish amorphous solids. Therefore, it can be stated that all studied samples are amorphous (glass solids) [9-11]. The existence of two humps in XRD, as seen in Figure 1, may be an indication of the genesis of two dissimilar micro-nucleating agents (regulate and control crystallinity) Zn (about $29.5°$) and Bi (about $51.8°$) all over the glass-matrix.
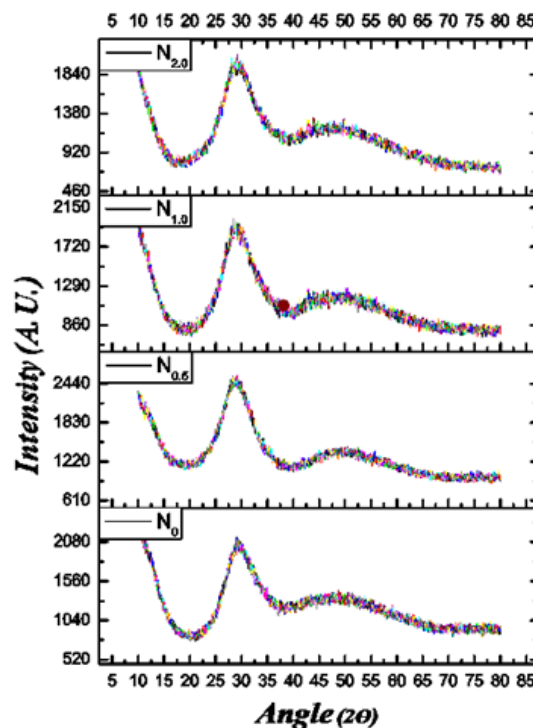

Figure 1. XRD Spectrogram for samples with codes N_0, $N_{0.5}$, $N_{1.0}$ and $N_{2.0}$.

Thermal analysis

Figure 2 (a, b, c, d) shows the DSC curves for samples with codes N_0, $N_{0.5}$, $N_{1.0}$ and $N_{2.0}$, respectively. All the DSC curves reveal an endothermic peak accompanied by the glass transition temperature (T_g). The T_g can be ascertained as the mid-point (point of inflection) of two temperatures, namely extrapolated onset temperature T_g^{on} and the extrapolated end temperature T_g^{end}. All the DSC curves exhibit two edged exothermic peaks attributes to the peak crystallization temperature indicated as T_{p1} and T_{p2}. The curves also exhibited two temperatures corresponding to the onset of crystallization, indicated as T_{c1} and T_{c2} [12, 13]. Corresponding to the two crystallization temperatures, only one glass (Sample Code N_0) batch ($20ZnO\text{-}40Bi_2O_3\text{-}40B_2O_3$) had two crystallization peak temperatures (T_{m1} and T_{m2}), and other batches except for N_0 had one crystallization peak temperature (T_{m1}).
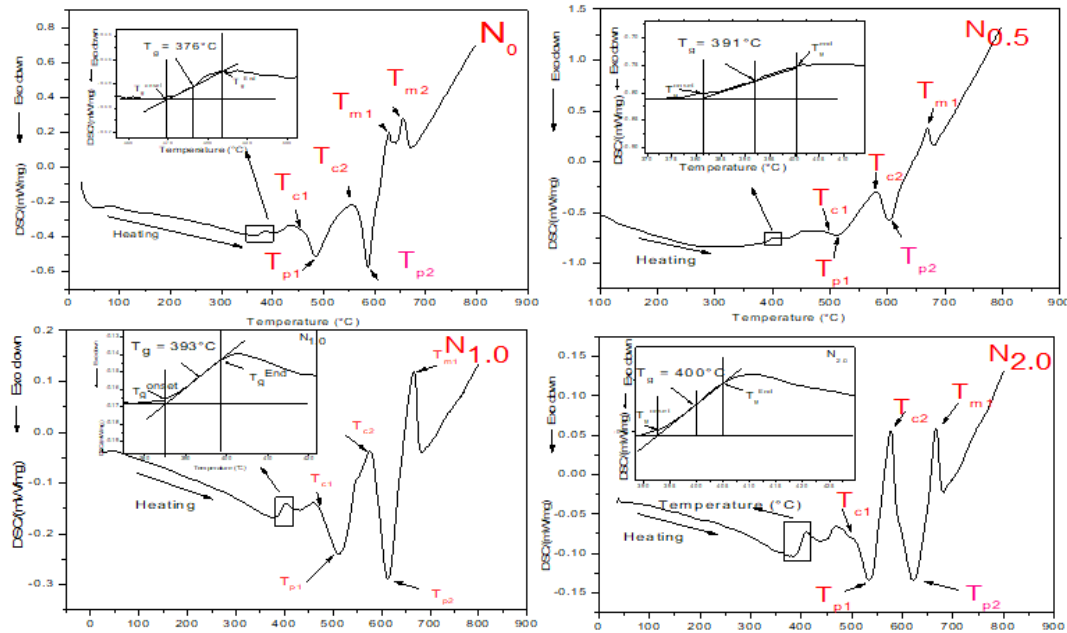

Figure 2. DSC curves for samples with codes N_0 (a), $N_{0.5}$ (b), $N_{1.0}$ (c) and $N_{2.0}$ (d).

All the above-mentioned parameters with their values obtained from DSC curves are listed in Table 2.

Table 2.
All the DSC parameters for sample with code N_0, $N_{0.5}$, $N_{1.0}$ and $N_{2.0}$ respectively.

Sample Code	T_g	T_{c1}	T_{c2}	T_{p1}	T_{p2}	T_{m1}	T_{m2}
N_0	376	452	557	486	585	626	657
$N_{0.5}$	391	499	581	512	602	671	–
$N_{1.0}$	393	471	575	514	614	667	–
$N_{2.0}$	400	502	577	536	622	666	–

Figure 3 shows that how the transition temperature was changed with the increment in the NiO fraction. It is conspicuous from the Table 2 and Figure 3 that the glass transition temperature and crystallization temperature increases

with the increase in the content of NiO. This direct effect of the concentration of NiO (which is a network modifier) on T_g values is observed as chemical bond modification between the glass former and modifier is involved while glass transition [14]. The value of T_g is highest for $N_{2.0}$, indicating the more the concentration of NiO results in more compacted glass structure [15]. Using the DSC data, the thermal stability of the glasses can be evaluated employing the equation by Dizetel [16]:

$$\Delta T = T_{c1} - T_g, \tag{1}$$

where ΔT represents the thermal stability, and the values obtained are 76, 108, 78 and $102°$C for N_0, $N_{0.5}$, $N_{1.0}$ and $N_{2.0}$, respectively. The glasses were having a value of ΔT greater than $100°$C are considered to be stable. The more the value of ΔT, the lesser is the tendency of glass for crystallization [16].
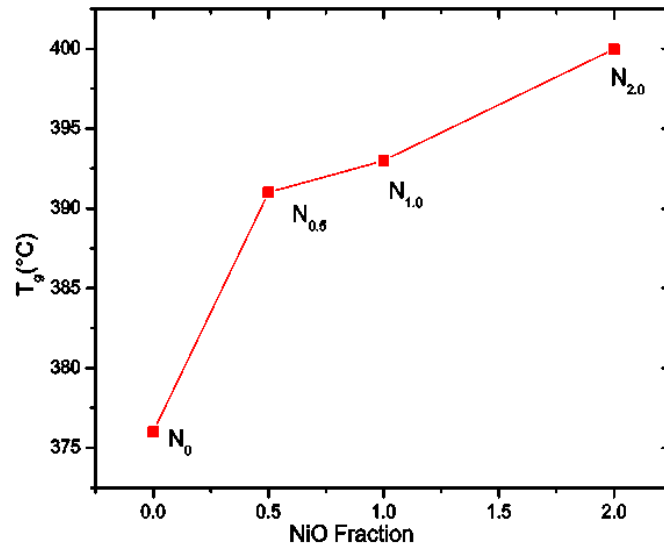

Figure 3. Transition temperature v/s NiO fraction.

FTIR Studies

The infrared absorption spectra of $xNiO$-$(20-x)$ ZnO-Bi_2O_3-B_2O_3 glass matrix are shown in Figure 4. Table 3 and Table 4 sum up the fundamental absorption bands observed in the studied glasses matrix and their vibration types, respectively. In the IR spectra of $xNiO$-$(20-x)ZnO$-Bi_2O_3-B_2O_3 glasses (Figure 4), as the content of NiO increases, the band at 521 cm^{-1}, contributing to the Bi-O-Bi vibration of distorted $[BiO_6]$ octahedral units [17, 18], results in increment of intensity and shift of wave-numbers towards lower. Since the $[BiO_3]$ polyhydra vibration band at 840 cm^{-1} [19-22] does not show any appearance in the IR absorption, it can be concluded that only $[BiO_6]$ octahedral units are the building blocks of bismuthate glass matrix. In contrast, we observed a more significant shift at the band from 679 to 696 cm^{-1}, which are related with the bending vibration of B-O-B in $[BO_3]$ units [19, 20]. This shift may be introduced by the electrostatic field of the intensely polarizing Bi^{2+} ions. The rising NiO content results in the increase of the electron cloud density around oxygen of $[BO_3]$ unit thus leads to an increase in the roll-torque of B-O-B band and consequently contributes to the bending vibration of B-O-B band shifts to a higher wavenumber.
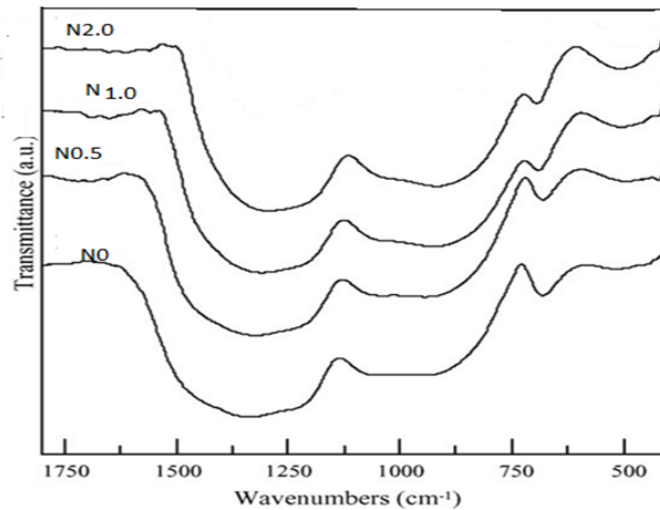
Figure 4. Infrared absorption spectra of xNiO-(20-x) ZnO- Bi_2O_3 - B_2O_3 glasses.

Table 3.
Observed IR absorption bands in xNiO-(20-x) ZnO- Bi_2O_3 - B_2O_3 glass system.

Glass Code	IR absorption bands (cm^{-1})			
N_0	1335	945	681	521
$N_{0.5}$	1325	943	681	494
$N_{1.0}$	1301	924	690	503
$N_{2.0}$	1290	918	694	507

The IR spectral range of 900-950 cm^{-1} is assigned for of [BO_4] units [21]. The existence of [BO_4] units in glass matrix shows that the addition of NiO to ZnO- Bi_2O_3 - B_2O_3 causes a cumulative transformation of [BO_3] units to [BO_4] units. Bands between 1200 and 1300 cm^{-1} are assigned to [BO_3] units [19, 20].

Table 4.
Vibration types of different IR wavenumbers.

Range of wave-numbers (cm^{-1})	Vibration types
420-520	Bi-O-Bi vibration of [BiO_6] octahedral units [17, 18]
680-720	Bending vibration of B-O-B in [BO_3] triangles [19, 20]
900-950	Stretching vibration of [BO_4] units [21]
1200-1300	Stretching vibration of B-O-B in [[BO_3]] triangles [19, 20]

As the NiO content increased, the intensity of both the bands decreases and a shift towards lower wave-numbers is observed. This is explained by capitulation the assumption that by the inducement of intensely polarizing Ni^{2+} ions a new bridging bond of Bi-O-B is formed. Since the stretching force constant of Bi-O bonding is substantially less than that of the B-O, the stretching frequency of Bi-O-B might tend to the lower side.

Conclusion

Thermal and structural properties of glass system xNiO-(20-x) ZnO- $40Bi_2O_3$ - $40B_2O_3$ have been studied. The amorphousity of glass samples was confirmed by XRD analysis. The result revealed the addition of NiO into the glass system increase the transition temperature of the glass system. The FTIR absorption spectra show that bismuth ions are incorporated in the glass network in BiO_3 pyramidal and BiO_6 octahedral units, and boron ions are incorporated in BO_3 and BO_4 units. The intensity of absorption bands of these structural units suggests that the structure of the glass matrix is very stable and is influenced by the presence of NiO ions.

References

[1] H. Rawson, Inorganic glass-forming systems (Academic Press, London, 1967) 317 p. [*WebLink*]

[2] M.Y. Hassaan et al., J. of Mat. and Appl. **9**(1) (2020) 46-54. [*CrossRef*]

[3] J. Krogh-Moe, Acta Crystallographica **15**(3) (1962) 190-193. [*CrossRef*]

[4] J. Lorosch et al., J. of Non-Cryst. Solids **69**(1) (1984) 1-25. [*CrossRef*]

[5] S. Hazra, A. Ghosh, Phy. Rev. B **51**(2) (1995) 851. [*CrossRef*]

[6] S. Hazra et al., Phy. Rev. B **56**(13) (1997) 8021. [*CrossRef*]

[7] S. Chakraborty, V. Sivasubramanian, Journal of Alloys and Compounds **747** (2018) 879-885. [*CrossRef*]

[8] W. H. Dumbaugh, Physics and Chemistry of Glasses **27**(3) (1986) 119-123. [*CrossRef*]

[9] A.C. Larson, R.B. Von Dreele, General Structure Analysis System, Los Alamos National Laboratory Report LAUR 86-748 (2000). [*WebLink*]

[10] S. Lanfredi et al., Journal of Solid State Chemistry **184**(5) (2011) 990-1000. [*CrossRef*]

[11] R.S. Kundu et al., Journal of Alloys and Compounds **587** (2014) 66-73. [*CrossRef*]

[12] B.-S. Kim et al., Journal of the European Ceramic Society **27**(2-3) (2007) 819-824. [*CrossRef*]

[13] W. Guo et al., Journal of the European Ceramic Society **37**(3) (2017) 1073-1081. [*CrossRef*]

[14] K. Jha, M. Jayasimhadri, Journal of the American Ceramic Society **100** (2017) 1402-1411. [*CrossRef*]

[15] J.A. Wilder, J.E. Shelby, Journal of the American Ceramic Society **67** (1984) 438-444. [*CrossRef*]

[16] A.-M. Yousefi et al., Nanotechnology Reviews, **3**(6) (2014) 527-552. [*CrossRef*]

[17] S. Bale et al., Journal of Alloys and Compounds **460**(1-2) (2008) 699-703. [*CrossRef*]

[18] M.E. Lines et al., Journal of Non-Crystalline Solids **89**(1-2) (1987) 163-180. [*CrossRef*]

[19] E.I. Kamitsos et al., Journal of Non-Crystalline Solids **126**(1-2) (1990) 52-67. [*CrossRef*]

[20] A.K. Hassan et al., Journal of Non-Crystalline Solids **172-174** (1994) 154-160. [*CrossRef*]

[21] G. El-Damrawi, K. El-Egili, Physica B: Condensed Matter **299**(1-2) (2001) 180-186. [*CrossRef*]

[22] R. Iordanova et al., Journal of Non-Crystalline Solids **180**(1) (1994) 58-65. [*CrossRef*]